공학석사 학위논문

# A study on optimal reference sensor placement for active control of road noise based on coherence analysis

## 노면소음 능동제어를 위한 상관성 기반 최적 센서 위치 선정 기법

2021 년 8 월

서울대학교 대학원

기계공학부

박 윤 설

# A study on optimal reference sensor placement for active control of road noise based on coherence analysis

## 노면소음 능동제어를 위한 상관성 기반 최적 센서 위치 선정 기법

지도교수 강 연 준

이 논문을 공학석사 학위논문으로 제출함

2021 년 4 월

서울대학교 대학원

기계공학부

박 윤 설

박윤설의 공학석사 학위논문을 인준함

2021 년 6 월

위 원 장 : 도 형 록

부위원장 : 강 연 준

위 원 : 김 도 년

# ABSTRACT

# A study on optimal reference sensor placement for active control of road noise based on coherence analysis

Yun Seol Park

School of Mechanical Engineering

The Graduate School

Seoul National University

Road noise is the primary noise source of vehicles and is directly related to vehicle noise, vibration, and harshness (NVH) performance. To attenuate vehicle interior noise caused by such tire–road interactions, the active noise control (ANC) strategy has been applied in the automotive industry. A set of reference sensors is included in active road noise control (ARNC) systems, and it is important to determine the locations of the sensors to accurately identify the transfer path of vibrations that induce road noise. In other words, it is necessary to maximize the performance of the ARNC system by finding optimal sensor locations among numerous candidate points on the vehicle. The trial-and-error method is time consuming for the selection of the final sensor set because it evaluates the noise

reduction for all possible sensor combinations. This study proposes a method to determine the subset of reference sensor locations using the correlation between signals and the Fisher information matrix. The proposed method selects the sensor with the highest correlation with vehicle interior noise as the first element of the subset. The subset is expanded in such a way that the next sensor is iteratively selected as a measure of the determinant of the coherence information matrix. This methodology can reduce the computational cost of performing a simulation because the initial sensor set consists only of signals that are highly correlated with the output signals. In addition, the simulation results yielded a reduction in road noise of approximately 7 dBA, which corresponds to an error within 0.2 ΔdBA of the target noise reduction.

**Keyword : Active road noise control, Optimal sensor placement, Effective independence method, Coherence function, Fisher information matrix**

**Student Number : 2019-22509**

# TABLE OF CONTENTS

# LIST OF TABLES

# LIST OF FIGURES

# CHAPTER 1

# INTRODUCTION

The active noise control (ANC) strategy is based on the superposition principle of two acoustical waves from the primary and secondary sources. When the two waves are out of phase and have the same amplitude, a quiet zone is generated by superposition and the complete cancellation of them. The traditional passive noise control approach increases the weight and volume because of the addition of sound absorbing materials, and it is effective only in the high-frequency range. To address these difficulties, the ANC approach is developed because it reduces noise with low weight and volume, and yields an excellent performance for low-frequency noise.

In view of the focus on cabin silence conditions and the use of light-weight materials in the automotive industry, the ANC strategy is recognized as a promising solution for the control of vehicle interior noise. The ANC applied to existing vehicles was largely limited to engine noise, because its timing and the extent of occurrence can be predicted [1–5]. Conversely, road noise control has only recently been considered because of the numerous variables involved. The road noise occurs when the vibration generated by the contact between the tire and pavement is transferred to the vehicle cabin through the tire, suspension, and vehicle body. It falls within the low-frequency range of 500 Hz or less, because it is transmitted by the structure-borne transfer path. In other words, road noise can be effectively controlled

through the ANC approach.

Several studies have been conducted on the active road noise control (ARNC) over the past 20 years. These studies have mainly focused on the introduction or development of adaptive filter algorithms for control systems [6–12] and the improvement of the convergence rate of the algorithm [13, 14]. All types of ARNC systems show good control performance only if the reference signals are well correlated to the targeted noise. Therefore, another important issue associated with noise reduction pertains to the determination of the optimal locations and the number of acceleration sensors. Because the reference sensors must detect all independent noise sources, the number of accelerometers should be at least greater than the independent degrees of freedom related to road noise [6]. In previous studies, independent noise sources were identified based on frequency domain approaches, such as principal component analysis [6, 15, 16] and coherence analysis [17, 18]. Meanwhile, the locations of sensors were determined on the basis of achievable performance, which was estimated with the use of the multiple coherence (MCOH) between the reference signals from accelerometers and the targeted road noise [6, 9, 11, 19]. However, this process can only predict the ARNC performance in the case in which the combination of sensors with best MCOH does not always lead to maximum noise reduction. In addition, as the positions of the candidate sensor increase, it takes a considerable amount of time to simply predict the ARNC performance for all configurable combinations. Therefore, a systematic and standardized method is needed to determine the optimal reference sensor locations

of the ARNC systems.

The existing influential and commonly used optimal sensor placement method is the effective independence (EFI) method proposed by Kammer [20–22]. The EFI method iteratively selects the candidate sensor locations that maximize their linear independence while including sufficient information on the target mode. The EFI method has been investigated and developed extensively by many scholars, and has been mainly applied to the modal analysis of large structures, such as bridges and spacecrafts [23–25]. However, only a few studies have adopted this method in the automotive industry, especially in the field of ARNC. In this study, a method is proposed for the determination of the subset of reference sensor locations by applying the EFI method while ensuring noise reduction levels similar to the target value of the ARNC system. This methodology starts with one acceleration sensor that has the highest correlation with the output acoustic signals. The next sensor that adds the largest amount of correlation information to the currently expanded sensor set is selected using the Fisher information matrix (FIM). When the elements of the subset are iteratively increased to reach the desired number of sensors, an ARNC simulation was performed on the configured sensor combinations. The simulation process includes Wiener filtering to calculate the level of noise reduction, which in turn accurately evaluates the ARNC performance. This methodology significantly reduces the time required to find the optimal sensor set with the best ARNC performance because it selects subsequent sensors by considering the coherence of the already determined reference sensors. To verify the feasibility of this

methodology, it was compared with the results of the trial-and-error and conventional methods.

This paper is organized as follows. In Section 2, the working process of the ARNC system is presented, including the Wiener filter and the theory of the coherence analysis. In Section 3, the conventional method that is used to predict the ARNC performance is introduced, and a coherence-based sensor set expansion (CSE) method is proposed. Subsequently, a case study is conducted to validate the proposed method, which is described in Section 4. The ARNC simulation results are discussed in three cases: 1) global maximum noise reduction (GMNR) for all combinations of candidate sensor locations, i.e., maximum achievable noise reduction, 2) noise reduction when selecting reference sensors based on conventional method, and 3) local maximum noise reduction when selecting reference sensors by applying the CSE method. Finally, conclusions and recommendations are provided in Section 5.

# CHAPTER 2

# THEORY

## 2.1 Active road noise control

The ARNC strategy actively reduces noise by analyzing various noise types from the road surface when the vehicle drives at middle or high speed and emitting sound waves that are inverted to noise in real time. Figure 2.1 presents the ARNC system. The system consists of acceleration sensors, amplifiers, microphones, loudspeakers, in conjunction with a digital signal processor (DSP), which is used for acoustic signal analysis. To simplify the system, an audio system that was already embedded in the vehicle was used rather than separate loudspeakers. The schematic of the working process of the ARNC system is shown in Figure 2.2. The primary path consists of the acoustic response from the noise source to the microphones. The accelerometers are located within the transfer paths of the vibration that causes road noise. The obtained vibration information is input to the DSP as the reference signal. The DSP analyzes this vibration to predict the interior noise and generates a control signal, which is the sound wave that is inverted to noise. The control signal is converted to an acoustic signal at the speaker, and the transfer path from the speaker to the microphone is the secondary path. A quiet zone is then created in the cabin as a result of the superposition of the primary and secondary sources. To check whether the

noise is reduced, the microphones installed in the cabin concurrently monitor the noise cancelation status in real time and send an error signal to the DSP. Based on this error signal, the DSP constantly tunes the control signal to minimize the error, and the noise of the driver's seat, the passenger seat and rear seats is gradually reduced. In conclusion, it is important for the ARNC system to find the optimal locations of the sensors to generate the appropriate control signal similar to the vibration source, while minimizing the time required for computations and measurements.

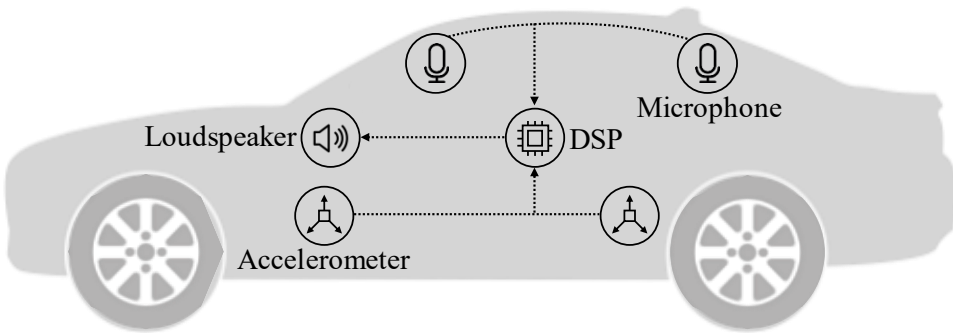


**Figure 2.1** System of active road noise control.

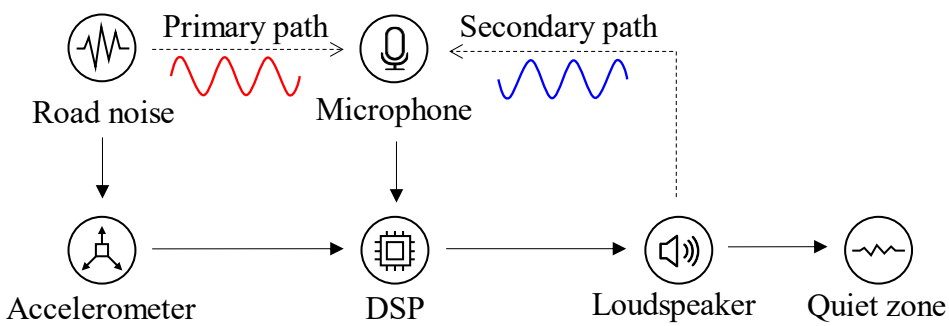


**Figure 2.2** Schematic of the working process of the active road noise control (ARNC) system.

## 2.2 Wiener filter

The DSP generates the control signal based on the use of an adaptive filter that changes the configuration of the controller according to changes in the system environment. The adaptive filter adjusts its parameters to respond accurately to a certain signal. Figure 2.3 presents a simple block diagram of the adaptive filter. In this figure, *P* is the primary path, *W* is the adaptive filter, and *C* is the secondary path. Herein, $x(n)$, $d(n)$, and $e(n)$ are the reference signal, desired response, and the error signal for the $n$th sample, respectively; $n$ denotes the number of samples in the time order of the digital signal. The filter coefficients are continually updated using input, output, and target signals.

In this study, the noise reduction in the ARNC system was evaluated with the use of a Wiener filter, which is known as the linear optimum discrete time filter. The Wiener filter is designed to generate an estimated output signal $y(n)$ with the use of a related input signal [26]. The filter output at a discrete time $n$ is defined by the linear convolution sum, as shown in Eq. (2.1),

$$y(n) = \sum_{k=0}^{\infty} w_k^* \, x(n-k), \tag{2.1}$$

where the asterisk denotes complex conjugation, $w_k$ is the $k$th filter coefficient, and $x(n-k)$ is the $k$th filter input. To optimize the filter design, the sum of the

mean–square values of each error between the estimated signal in Eq. (2.1) and the target signal should be minimized. The cost function $J$, which is the index of performance, is defined as the mean square error, as shown in Eq. (2.2),

$$J = E\left[\sum_{l=1}^{L} e_l^2(n)\right], \tag{2.2}$$

where $L$ is the number of microphones, $e(n)$ is the estimation error defined as $d(n) - y(n)$, which is the difference between the desired response and the actual response, and $E$ represents the statistical expectation. The filter coefficient $w$ is adjusted by applying the gradient operator $\nabla$ to the cost function $J$, and a solution is found such that all the elements of the gradient vector $\nabla J$ simultaneously equal to zero, as shown in Eq. (2.3),

$$\nabla J_k = 0, \qquad k = 0, 1, 2, \cdots. \tag{2.3}$$

The ARNC simulation is performed on the basis of this Wiener filter, and the sensor combination with the best noise reduction result is determined as the optimal reference sensor set.

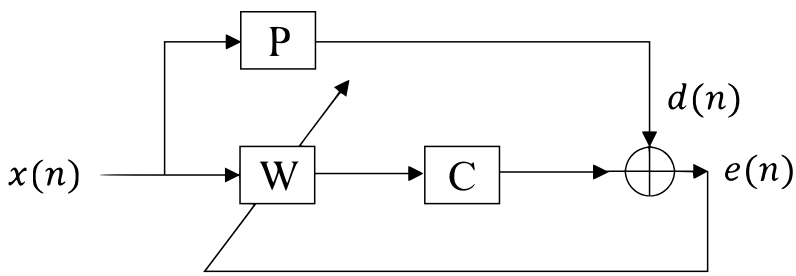


**Figure 2.3** Simple block diagram of adaptive filter.

## 2.3 Coherence analysis

Traditionally, coherence analysis is a useful tool for optimal sensor placement. It helps examine the relationships between two signals or datasets in different physical processes, including vibration and acoustic signals. From the NVH point of view, a single coherence (SCOH) for each vibro–acoustic path is evaluated to identify the location on the structure highly correlated with the road noise bands in the ARNC system. The SCOH between input $x(t)$ and output $y(t)$ in a single-input/single-output system is defined as follows:

$$\gamma_{xy}^2(f) = \frac{\left|S_{xy}(f)\right|^2}{S_{xx}(f)S_{yy}(f)} \tag{2.4}$$

and satisfies $0 \leq \gamma_{xy}^2(f) \leq 1$ for all $f$ values. In this equation, $S$ denotes the spectral density function, which was calculated by the fast Fourier transform of the corresponding correlation function. In this study, the SCOH was calculated with the use of the acceleration signals measured from the vehicle chassis and the sound pressure level (SPL) signals inside the vehicle as input and output signals, respectively. A coherence map illustrated the correlation of each vibro–acoustic path in the 0–500 Hz frequency band, and the sensor corresponding to the position with the highest value was determined as the first element of the subset.

In a multiple-input/single-output system, as shown in Figure 2.4, the MCOH

between a series of input signals and one output signal is used as another statistical indicator to analyze the correlation of a given dataset. In this figure, $q$ is the number of input signals and $H_i$ represents the transfer function of the $i$th input signal to the output signal. The multiple coherence function between the series of inputs $x(t) = \{x_1(t), \cdots, x_q(t)\}$ and the output $y(t)$ is defined as follows:

$$\gamma_{y:x}^2(f) = 1 - \left(\frac{|\mathbf{S}_{yxx}(f)|}{S_{yy}(f)|\mathbf{S}_{xx}(f)|}\right). \tag{2.5}$$

Herein, the input spectral density matrix $\mathbf{S}_{xx}(f)$ is a $q \times q$ matrix, defined as follows:

$$\mathbf{S}_{xx}(f) = \begin{bmatrix} S_{11} & S_{12} & \cdots & S_{1q} \\ S_{21} & S_{22} & \cdots & S_{2q} \\ \vdots & \vdots & & \vdots \\ S_{q1} & S_{q2} & \cdots & S_{qq} \end{bmatrix}. \tag{2.6}$$

An augmented spectral density matrix $\mathbf{S}_{yxx}(f)$ of the output $y(t)$ with the inputs $x_i(t)$ is the $(q+1) \times (q+1)$ matrix, expressed as follows:

$$\mathbf{S}_{yxx}(f) = \begin{bmatrix} S_{yy} & S_{y1} & S_{y2} & \cdots & S_{yq} \\ S_{1y} & S_{11} & S_{12} & \cdots & S_{1q} \\ S_{2y} & S_{21} & S_{22} & \cdots & S_{2q} \\ \vdots & \vdots & \vdots & & \vdots \\ S_{qy} & S_{q1} & S_{q2} & \cdots & S_{qq} \end{bmatrix}. \tag{2.7}$$

For the relationship between SCOH and MCOH, the MCOH is the sum of the SCOH between each input and output only if the input signals are independent of each other. In other words, when the input signals are correlated with each other, MCOH should be calculated according to Eq. (2.5). The ARNC system requires a series of acceleration sensors to be optimally placed to help the DSP generate an appropriate control signal. Previous studies have shown that the number of reference sensors should be as small as possible to simplify the control structure and reduce the computational burden. The performance is improved when the MCOH between a series of inputs and output is close to one [19]. In general, the MCOH tends to improve when each of the input signals has a high SCOH value for the output signal [27].

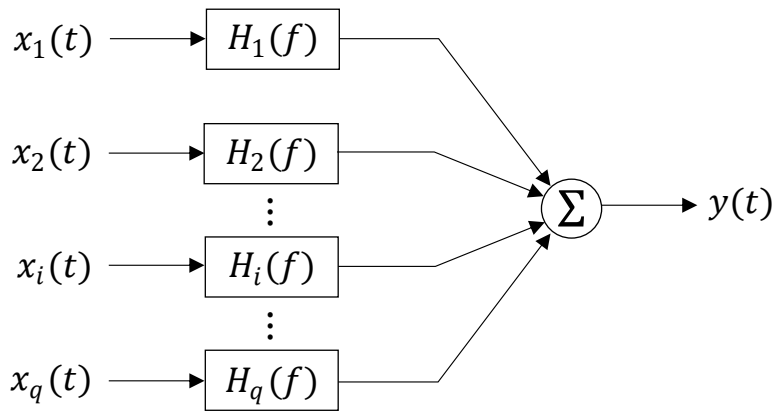


**Figure 2.4** Multiple-input/single-output system.

# CHAPTER 3

# METHODOLOGY

In this study, a total of 18 candidate sensor locations were initially specified based on considerations of the transfer path of the road noise, of which four reference signals were required for the ARNC system. Thus, four of the 18 positions were selected, and the corresponding signals were input to the DSP. Meanwhile, eight error microphones were installed inside the vehicle. In this section, coherence analysis is performed using the vibration response at the vehicle chassis as the input and the vehicle interior noise from microphone as the output.

## 3.1 Conventional method

The conventional method directly selects the sensor combination that gives the best MCOH with the interior noise. This method assumes that the MCOH value and ARNC performance are directly related, and that as the value of the MCOH increases, the greater is the noise reduction.

For 18 candidate sensor response vectors $x_1(t), x_2(t) \cdots, x_{18}(t)$, the signal set of one specific sensor combination $x(t) = \{x_1(t), x_2(t), x_3(t), x_4(t)\}$ is considered. The desired response vectors from eight microphones are

$y_1(t), y_2(t) \cdots, y_8(t)$, respectively. The multiple coherence function between the series of inputs $x(t)$ and $j$th output $y_j(t)$ is as follows:

$$\gamma^2_{y_j:x}(f) = 1 - \left( \frac{\left|\mathbf{S}_{y_j xx}(f)\right|}{S_{y_j y_j}(f)|\mathbf{S}_{xx}(f)|} \right). \tag{3.1}$$

In this equation, because the multiple coherence functions are constructed for each of the eight output signals, the final MCOH value is derived by averaging these values per frequency as follows:

$$\gamma^2_{y:x}(f) = \frac{\sum_{j=1}^{8} \gamma^2_{y_j:x}(f)}{8}. \tag{3.2}$$

For all 3060 sensor combinations selecting four out of 18 candidate sensors, each MCOH was calculated by repeating the aforementioned process. The locations of the sensor set with the best MCOH were finally selected, and the ARNC simulation with the Wiener filter was performed with the use of this set of signals as the input.

## 3.2 CSE method—coherence-based sensor set expansion method

This method is an application of the EFI method, which is mainly used for optimal candidate sensor placement to predict the mode shape of large structures, such as bridges and spacecrafts. In the ARNC system, it is necessary to minimize the error signals from the microphones by generating the control signal on the basis of the accurate estimation of interior noise, which is given as

$$P = E[(y - \hat{y})(y - \hat{y})^T] = Q^{-1}, \tag{3.3}$$

where $P$ is the covariance of the estimated error, $y$ is the desired response from the microphone, $\hat{y}$ is the response estimated by the DSP, and $Q$ is the FIM, which is the inverse matrix of the error covariance matrix. Maximizing $Q$ implies the minimization of the corresponding error covariance matrix, and thus yields the best estimation. According to [20–22], the EFI method uses the determinant as a measure and evaluates the contribution of each sensor location to the determinant. Because the measured noise signals are assumed to be independent and have identical statistical properties, the FIM can be expressed as follows:

$$Q = \varphi^T \varphi\,, \tag{3.4}$$

where $\varphi$ is a single or multiple coherence function in this study. Using this FIM, the candidate sensor subset is iteratively expanded by choosing the next sensor that adds the largest amount of correlation information to the previous set.

First, the SCOH between the input and output signal is analyzed, and an initial sensor set is constructed starting with the candidate sensor that gives the best SCOH value. For the $i$th input $x_i(t)$, the SCOH with the $j$th output $y_j(t)$ is expressed in a similar manner to the one in Eq. (2.4):

$$\gamma_{x_i y_j}^2(f) = \frac{\left|S_{x_i y_j}(f)\right|^2}{S_{x_i x_i}(f) S_{y_j y_j}(f)}. \tag{3.5}$$

In this equation, because the single coherence functions are constructed for each of the eight output signals, the final SCOH for $x_i(t)$ is derived by averaging these values per frequency as follows:

$$\gamma_{x_i y}^2(f) = \frac{\sum_{j=1}^{8} \gamma_{x_i y_j}^2(f)}{8}. \tag{3.6}$$

This process was repeated for all 18 input signals, and the SCOH of each sensor was calculated. The sensor that gave the best SCOH value was selected. The following process was performed to select the next sensor that adds the largest amount of correlation information while considering the coherence of this starting sensor.

The FIM of the initial sensor set with one element was composed of multiple

coherence functions, as follows:

$$Q_o = \varphi_o^T \varphi_o = \{\gamma_{y:x}^2(f)\}^T \gamma_{y:x}^2(f), \tag{3.7}$$

where $x = \{x_p\}$ is the input, $p$ is the position number of the starting sensor, and $y = \{y_1, y_2 \cdots, y_8\}$ represents the eight outputs. As shown by Eqs. (3.1) and (3.2), MCOH is the average of eight values calculated between the input $x_p$ and one output $y_j$. For all remaining sensors except the starting sensor, the amount of information added to the currently expanded sensor set was calculated as follows:

$$Inf_i^+ = \det\left(\varphi_i Q_o^{-1} \varphi_i^T\right). \tag{3.8}$$

Herein, $Inf_i^+$ represents the amount of new correlation information added by the $i$th sensor, and $\varphi_i$ is the single coherence function between the $i$th input $x_i$ and outputs $y = \{y_1, y_2 \cdots, y_8\}$ defined by Eqs. (3.5) and (3.6) as follows:

$$\varphi_i = \gamma_{x_i y}^2(f) = \frac{\sum_{j=1}^{8} \gamma_{x_i y_j}^2(f)}{8}. \tag{3.9}$$

Once the $Inf^+$ values were calculated for the 17 remaining sensors, they were ranked, and the location of the highest ranked sensor was added to the initial candidate sensor set so that the coherence information was incremented by the

maximum amount.

Thus, at this stage, the two locations of the initial sensor set had been determined, and the position of the third sensor was also selected according to the aforementioned process. As shown in Eq. (3.7), the FIM of the initial sensor set was composed of multiple coherence functions. The only difference is that the input signal set was expanded to two with $x = \{x_p, x_q\}$, where $q$ is the position number of the second sensor. After composing a new $Q_o$ through the MCOH between the two inputs and each output, $Inf^+$ was calculated for each of the 16 remaining sensors, with the exclusion of the two sensors that had already been selected. These values were ranked, and the location of the sensor with the largest value was added to the candidate sensor subset as a third element. Similarly, the remaining sensors were re-ranked, and the highest ranked sensor was added as a fourth element to the candidate sensor subset. By iterating through this process, new sensors were added to the initial candidate set one at a time, and were expanded until the desired number $n$ was attained. Because four reference signals were required in the ARNC system, $n$ should be at least four or more. When a candidate sensor subset consisting of $n$ elements is determined, ${}_n\mathrm{C}_4$ sensor combinations that select four out of $n$ are configurable. In other words, these combinations are part of the total of 3060 sensor combinations that select four out of 18 candidate sensors. For each of these sensor combinations, the ARNC simulation was performed to compare the noise reduction level. Finally, the sensor combination with the best performance was determined and the corresponding noise reduction level was recorded.

# CHAPTER 4

# CASE STUDY

## 4.1 Experimental and analytical procedure

This section describes the procedure for measuring vibration responses and SPL signals through vehicle experiment, as well as the data analysis process. First, to measure the acceleration responses of the vehicle chassis under operating conditions, 18 accelerometers were used. The road noise was transmitted by the structure-borne transfer paths. Thus, the accelerometers were attached to major components of the vibration transfer paths of the vehicle to acquire vibration signals that induce road noise. A total of 16 acceleration sensors were located on the subframe mounts, knuckles, and dampers on the front and rear of the chassis; two accelerometers were also located on both sides of the trailing arms of the multi-link suspension. In this way, a total of 18 candidate input signals were obtained initially at the main force input points of the vehicle.

As shown in Figure 4.1, a total of eight error microphones were installed in the driver's seat, the passenger seat and rear seats to measure the interior noise of the vehicle. The throughput time data were measured at three different driving speeds (50, 60, and 80 km/h) on the same road surface according to a sampling frequency of 2000 Hz. These driving conditions were adopted in consideration of the road noise,

which occurred when the vehicle was driven at middle or high speed. The power spectral density was obtained based on the calculation of the fast Fourier transform (FFT) on the measured acceleration signals and SPL data, respectively. The measurements were performed with FCEV crossover, which does not possess any engine noise.

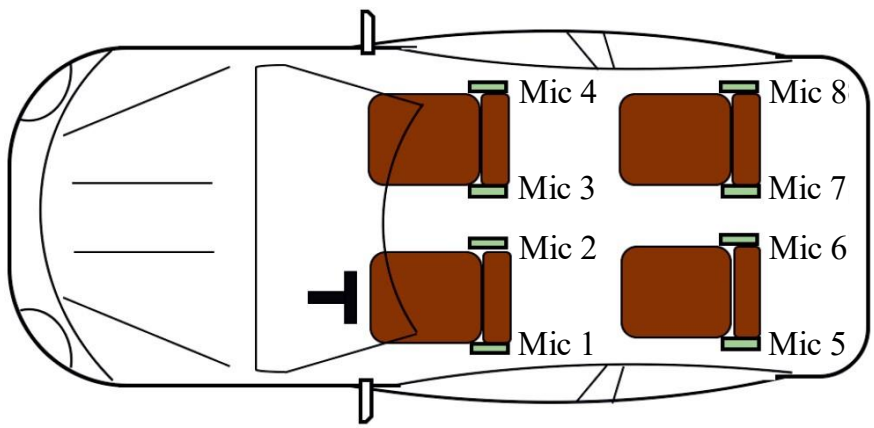


**Figure 4.1** Upper view of error microphone locations.

## 4.2 ARNC simulation

In this section, the accuracy, efficiency, and reliability of the two methods described in Section 3 were compared. First, all combinations were examined to establish the comparison criteria for noise reduction of the two methods. The accuracy was evaluated on the basis of the absolute error between the criteria and the results of each method, and the computational effort was compared by predicting the time required for the entire process. Finally, the reliability was verified by comparing the noise reduction level of the CSE method with GMNR in the 0–500 Hz frequency range. This frequency range was applied in all cases, including the coherence analysis and the interior noise evaluation. The final noise reduction values were derived by averaging the SPL reduction obtained from eight separate microphones for each frequency.

### 4.2.1 ARNC simulation with total sensor combinations

The maximum achievable noise reduction GMNR, was calculated by performing simulations with the Wiener filter for all sensor combinations. Therefore, a total of 3060, ${}_{18}C_4$ combinations were investigated for one driving condition, which required 102 hours to complete the simulation. The ARNC simulation results with the total sensor combinations are summarized in Table 4.1. Figure 4.2 shows the GMNR levels at microphone 2 under the three driving conditions.

**Table 4.1** Maximum achievable noise reduction level and corresponding sensor set for total combinations.

| | Driving condition | | |
|---|---|---|---|
| | 50 km/h | 60 km/h | 80 km/h |
| Global maximum noise reduction (GMNR) [ΔdBA] | 7.85 | 7.61 | 6.17 |
| Sensor set | 1, 8, 10, 18 | 4, 8, 10, 18 | 1, 8, 11, 16 |

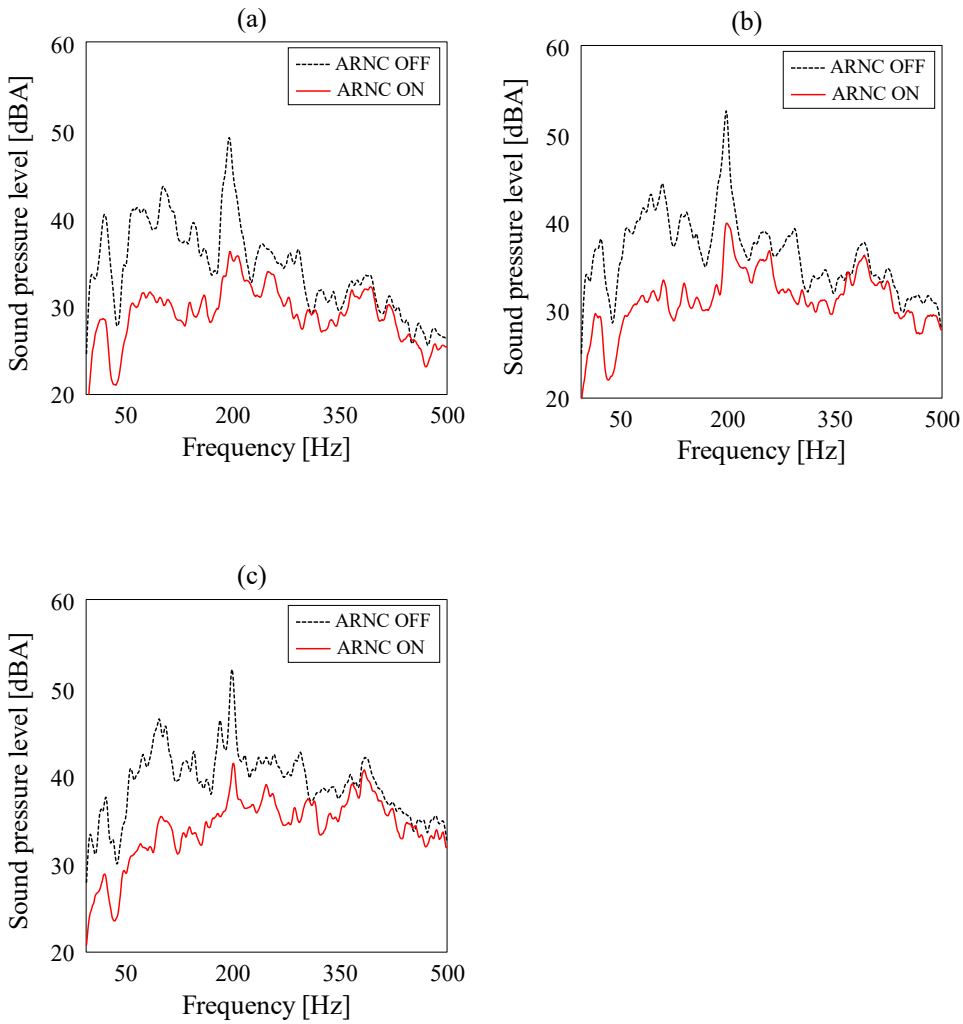


**Figure 4.2** Maximum achievable noise reduction levels of microphone 2 at the driving speeds of (a) 50 km/h, (b) 60 km/h, and (c) 80 km/h.

### 4.2.2 ARNC simulation for conventional method

The noise reduction level was estimated in the case of the conventional method, which selects a sensor set based on MCOH. It took 14 hours to calculate the MCOH for all 3060 sensor combinations in one driving condition. The obtained MCOH values were ranked, and the ARNC simulation was performed only for the top ranked sensor combination. Table 4.2 lists the simulated sensor combination and the corresponding noise reduction. In theory, the noise reduction is expected to be larger for sensor combinations with higher MCOH values. However, compared with the results of Table 4.1, the achieved GMNR was not directly related to the MCOH value. Figure 4.3 shows the MCOH of the 3060 combinations and the corresponding noise reduction. This indicates that the sensor combination with the highest MCOH does not represent the highest noise reduction, and only a positive correlation exists. Thus, to address this problem, a robust method for selecting a reference sensor set is required.

**Table 4.2** Noise reduction and sensor set for conventional method.

| | Driving condition | | |
|---|---|---|---|
| | 50 km/h | 60 km/h | 80 km/h |
| Noise reduction [ΔdBA] | 7.70 | 7.52 | 6.12 |
| Sensor set | 4, 8, 10, 16 | 4, 8, 11, 16 | 4, 8, 11, 16 |

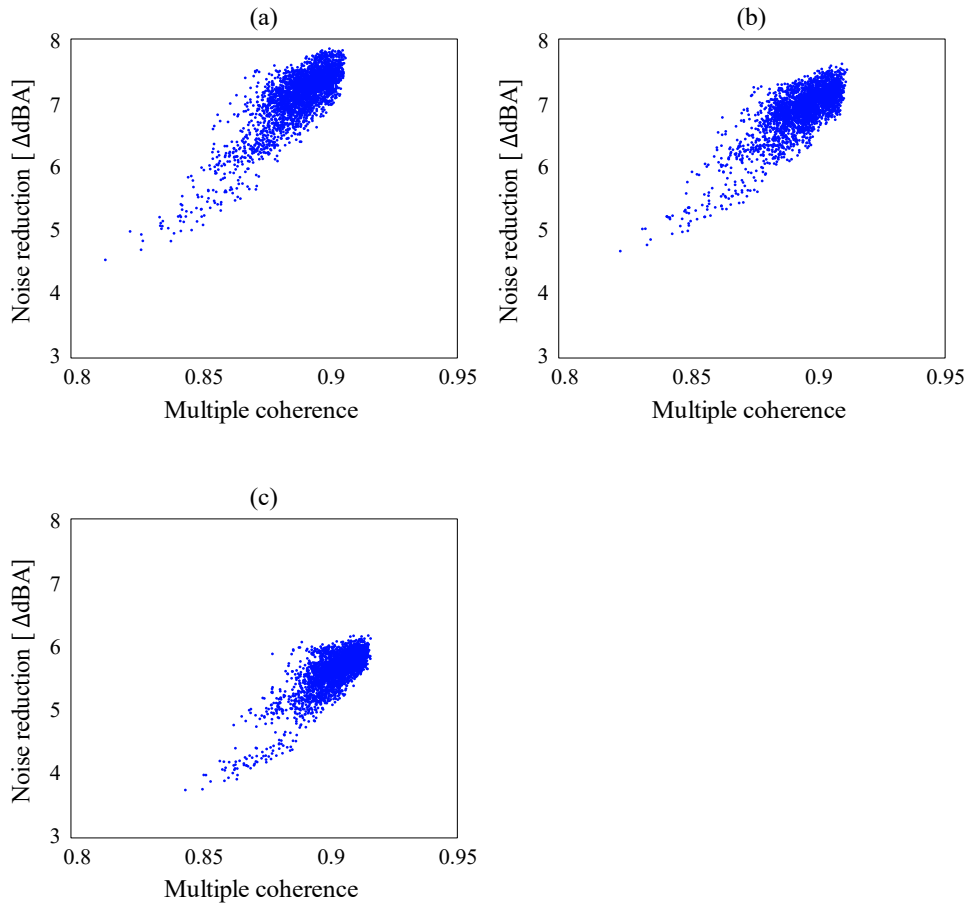


**Figure 4.3** Multiple coherence (MCOH) and corresponding noise reduction at the driving speeds of (a) 50 km/h, (b) 60 km/h, and (c) 80 km/h.

### 4.2.3 ARNC simulation for CSE method

The local maximum noise reduction level was evaluated with the use of the CSE method suggested in this study. The main purpose of the CSE method is to reduce the number of candidate sensors by eliminating unnecessary sensor locations among a large number of sensors. Similar to the EFI method, the contribution of each sensor to the target system was evaluated to obtain an optimal subset of sensor locations. The subset started with the sensor that gave the best SCOH value for the interior SPL signals, and it iteratively expanded in a way that the next sensors that added the largest amount of correlation information to the previous subset were selected. When the number of initial candidate subset reached the desired number $n$, the local maximum noise reduction for ${}_{n}\mathrm{C}_{4}$ sensor combinations was calculated. Table 4.3 lists the number of sensor combinations and the time required for all cases where $n$ ranges from four to eight. In column 3 of this table, the times listed included two processes: 1) determination of an optimal sensor subset expanded to the desired number $n$, 2) simulation of all sensor combinations for obtaining the local maximum noise reduction in that case. Figure 4.4 shows the SCOH of all 18 inputs for the frequency range of 0–500 Hz, which were obtained using Eqs. (3.5) and (3.6). As shown in this figure, the correlation of each vibro–acoustic path was compared with the use of the coherence map. In all three datasets, the candidate sensor position with the highest SCOH value was #10. Table 4.4 lists the expanded sensor subset for each iteration with #10 as the starting sensor. In column 2 of this table, the initial candidate

sensor set selected for each driving condition were the sensor positions in bold. Because more reference sensors were needed to predict the internal noise caused by the road noise when driving at high speeds, the desired numbers of the three data sets were 4, 5, and 7, respectively. Table 4.5 summarizes the ARNC simulation results performed for 1, 5, and 35 sensor combinations, respectively, as listed in Table 4.3. The last row of this table shows the time corresponding to each desired number in Table 4.3.

**Table 4.3** Number of sensor combinations and the time required according to the desired number.

| Desired number ($n$) | Number of sensor combinations (${}_nC_4$) | Time [hours] |
|---|---|---|
| 4 | 1 | 0.1 |
| 5 | 5 | 0.2 |
| 6 | 15 | 0.6 |
| 7 | 35 | 1.2 |
| 8 | 70 | 2.4 |

**Table 4.4** Expanded sensor set chosen by the coherence-based sensor set expansion (CSE) method.

| Driving condition | Expanded sensor set |
|---|---|
| 50 km/h | ***10***, ***8***, ***17***, ***4***, 13, 11, 9, 14 |
| 60 km/h | ***10***, ***5***, ***18***, ***6***, ***4***, 7, 3, 16 |
| 80 km/h | ***10***, ***5***, ***6***, ***17***, ***3***, ***2***, ***16***, 12 |

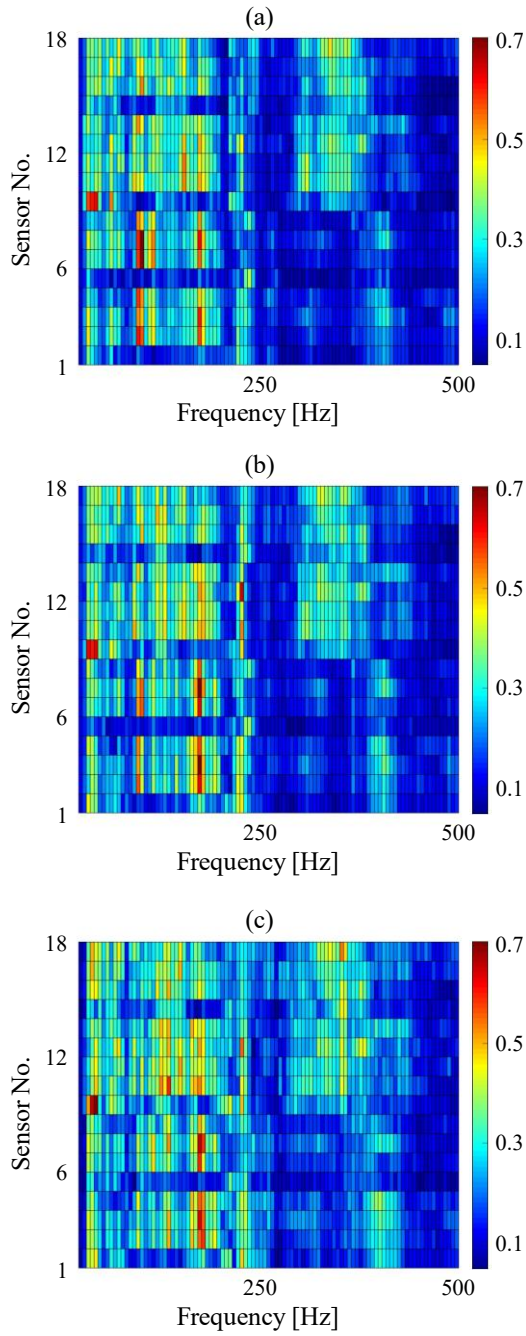


**Figure 4.4** Coherence map between 18 acceleration signals and microphones at the driving speeds of (a) 50 km/h, (b) 60 km/h, and (c) 80 km/h.

**Table 4.5** Local maximum noise reduction level and corresponding sensor set for CSE method.

| | Driving condition | | |
|---|---|---|---|
| | 50 km/h | 60 km/h | 80 km/h |
| Local maximum noise reduction [ΔdBA] | 7.79 | 7.55 | 6.01 |
| Sensor set | 4, 8, 10, 17 | 4, 5, 10, 18 | 2, 5, 10, 17 |
| Time [hours] | 0.1 | 0.2 | 1.2 |

# CHAPTER 5

# RESULTS AND DISCUSSION

The GMNR in Section 4.2.1 was used as the criterion for comparison of the two methods in Section 3. The accuracy was evaluated by calculating the absolute error between this criterion and the noise reduction results of each method. Table 5.1 lists the ARNC simulation results and corresponding errors. The reference sensor combination that was selected by the conventional method shows average noise reduction errors of 1.91, 1.18 and 0.81% for each driving condition within the frequency range of 0 to 500 Hz. The reference sensor combination that was selected by the CSE method yielded the average noise reduction errors of 0.76, 0.79, and 2.59 % for each driving condition within the same frequency range. Specifically, this method reduced the vehicle interior noise by approximately 7 dBA in all driving conditions, which corresponds to an error within 0.2 ΔdBA of the target noise reduction result. Figure 5.1 shows the local maximum noise reduction level at microphone 2 using the CSE method and the GMNR level together. This figure shows that the amount of the interior noise reduction at the driving speeds of 50 and 60 km/h is more similar to the GMNR than that at 80 km/h. It can be confirmed that the CSE method is effective and reliable in controlling the road noise generated in a broadband and not in a specific frequency range, because the absolute error evenly remains throughout the frequency range. In addition, it took 102 hours to find the

global optimal sensor combination; this resulted in a significant computational burden. The conventional method used to compensate for this drawback also took 14 hours to obtain the final sensor combination, which still needed efficiency improvement. By comparison, the CSE method took only 0.1–1.2 hours to determine the optimal sensor combination, which indicates that the computational effort was significantly reduced.

**Table 5.1** ARNC simulation results of each method – noise reduction level (absolute error).

| | | Driving condition | | |
|---|---|---|---|---|
| | | 50 km/h | 60 km/h | 80 km/h |
| Noise reduction (Error) [ΔdBA] | Global maximum | 7.85 (–) | 7.61 (–) | 6.17 (–) |
| | Conventional method | 7.70 (0.15) | 7.52 (0.09) | 6.12 (0.05) |
| | CSE method | 7.79 (0.06) | 7.55 (0.06) | 6.01 (0.16) |

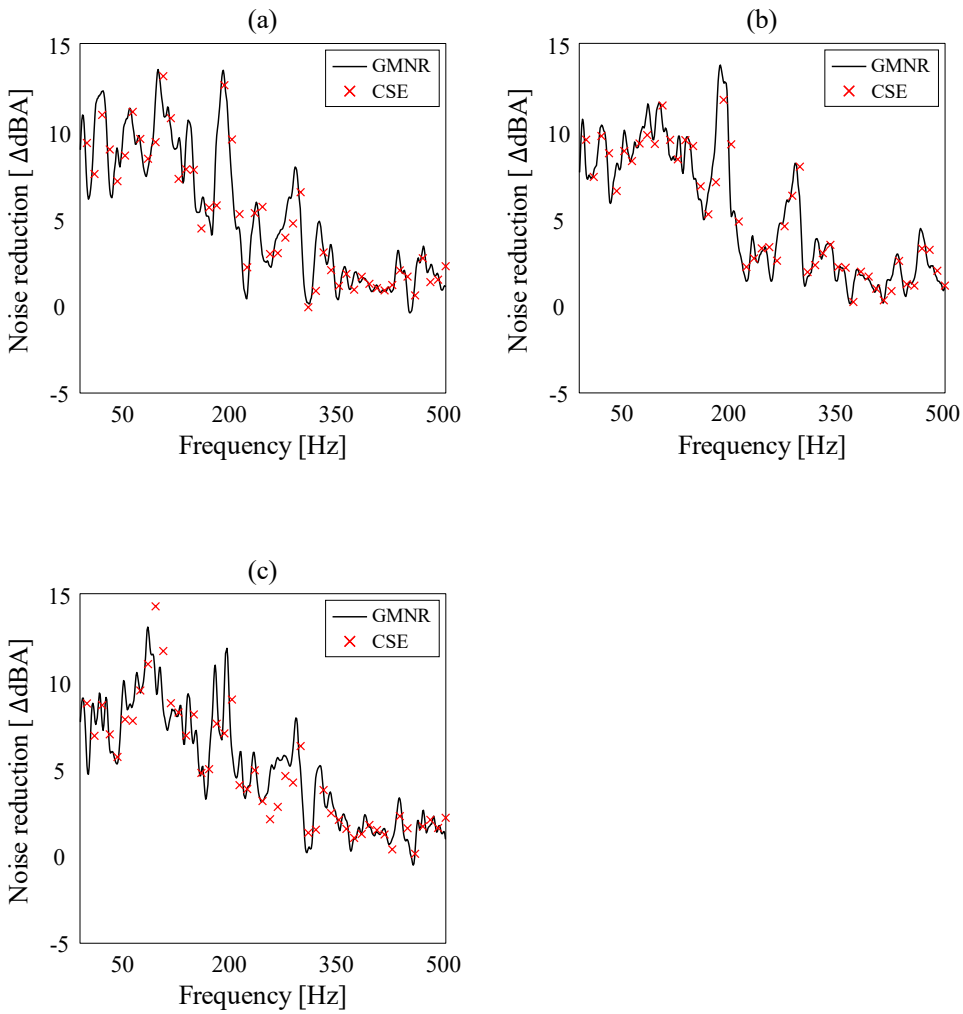


**Figure 5.1** Local maximum noise reduction at microphone 2 by CSE method at the driving speeds of (a) 50 km/h, (b) 60 km/h, and (c) 80 km/h.

# CHAPTER 6

# CONCLUSIONS

In this present study, the feasibility of coherence-based sensor set expansion for optimal sensor placement in ARNC system was studied. This method iteratively expanded an initial set of sensors based on the maximization of the determinant of the correlation information matrix. The results demonstrate that an optimal subset of sensor locations can be obtained by evaluating the contribution of each remaining sensors to the correlation information corresponding to the current expanding sensor set. The noise reduction level was directly calculated by performing simulations for all sensor combinations with the expanded sensor set to accurately verify the performance of the ARNC system. In the case study, it is confirmed that the CSE method tends to show greater noise reduction than the conventional method in three driving conditions where road noise is dominant. The level is approximately 7 dBA, which is largely consistent with the targeted noise reduction, and the absolute errors are within 0.2 dBA of GMNR in all driving conditions. In addition, the time required for a subset of five initial sensors was reduced to 0.2 h, compared with 102 and 14 hours for the trial-and-error and the conventional method, respectively. This indicates that the computational burden is also reduced with the CSE method compared with other prior methods.

A significant advantage of the proposed method is that the optimal sensor

locations were accurately and efficiently determined by eliminating unnecessary sensor positions. However, the initial candidate subset by the CSE method can be expanded only to the number of output signals, that is, the desired number $n$ was limited. If the number of sensors in the subset equals that of the output signals, all components of $\gamma_{y:x}^2$ in Eq. (3.7) become equal to one, $Q_o$ becomes a singular matrix, and $Inf_i^+$ in Eq. (3.8) is not calculated. In the case study presented herein, the local maximum noise reduction was achieved with a desired number smaller than the number of output signals. However, because road noise is associated with variables such as tire type, road condition, and driving speed, and has random nature, more initial candidate sensors may be needed if conditions are different from those in this case study. Therefore, in preparation for these cases, future research will be concentrated on the iterative selection of more initial candidate sensors, while maintaining the overall performance close to the GMNR.

Nevertheless, this study is a positive starting point toward an improved method that can overcome these drawbacks in the coming years. First, the proposed method has the potential to determine the optimal positions of reference sensors within a short time for automobile manufacturers who cannot attach a large number of sensors because of the cost inefficiency in the product development stage. Second, in addition to the low-frequency road noise noted in this study, the proposed method can be applied to the control of wind noise within a frequency range of 500–5000 Hz through further improvements. In addition, this method may be useful in other industries wherein optimal sensor placement is required for the correlation of any two signals.

# REFERENCES


[1] L.J. Oswald, Reproduction of diesel engine noise inside passenger compartments using active adaptive noise control, *Proc. Inter-Noise '84*, 483–488.

[2] S.J. Elliott, Active noise and vibration control in vehicles, In *Vehicle Noise and Vibration Refinement*, Woodhead Publishing, 2010, pp. 235–251.

[3] L.P. de Oliveira, K. Janssens, P. Gajdatsy, H. Van der Auweraer, P.S. Varoto, P. Sas, W. Desmet, Active sound quality control of engine induced cavity noise, *Mech. Syst. Signal Process*. 23 (2009) 476–488.

[4] J. Duan, M. Li, T.C. Lim, M.R. Lee, F. Vanhaaften, M.T. Cheng, T. Abe, Comparative study of frequency domain filtered-x LMS algorithms applied to vehicle powertrain noise control, *Int. J. Veh. Noise Vib*. 5 (2009) 36–52.

[5] J. Duan, M. Li, T.C. Lim, M.R. Lee, W. Vanhaaften, M.T. Cheng, T. Abe, Active control of vehicle transient powertrain noise using a twin-FxLMS algorithm, *J. Dyn. Syst. Meas. Control*. 133 (2011).

[6] T.J. Sutton, S.J. Elliott, A.M. McDonald, T.J. Saunders, Active control of road noise inside vehicles, *Noise Control Eng. J*. 42 (1994) 137–147.

[7] R. Bernhard, Road noise inside automobiles, *Proc. 1995 Int. Symp. Active Control of Sound and Vib.*, Newport Beach, CA, USA, (1995).

[8] W. Dehandschutter, J. Van Herbruggen, J. Swevers, P. Sas, Real-time enhancement of reference signals for feedforward control of random noise due to multiple uncorrelated sources, *IEEE Trans. Signal Process*. 46 (1998) 59–69.

[9] S.H. Oh, H.S. Kim, Y. Park, Active control of road booming noise in automotive interiors, *J. Acoust. Soc. Am*. 111 (2002) 180–188.

[10] C. Park, C. Fuller, M. Kidner, Evaluation and demonstration of advanced active noise control in a passenger automobile, *Proc. 2002 Int. Symp. Active Control of Sound and Vib.*, Southampton, UK, (2002).

[11] J. Duan, *Active Control of Vehicle Powertrain and Road Noise* (Doctoral dissertation, University of Cincinnati), 2011.

[12] J. Cheer, S.J. Elliott, The design and performance of feedback controllers for the attenuation of road noise in vehicles, *Int. J. Acoust. Vib*. 19 (2014) 155–164.

[13] C.M. Heatwole, R.J. Bernhard, Reference transducer selection for active control of structure-borne road noise in automobile interiors, *Noise Control Eng. J*. 44 (1996) 35–43.

[14] M. Akiho, M. Haseyama, H. Kitajima, A practical method to reduce a number of reference signals for the ANC system, *ICASSP99 (Cat. No. 99CH36258)*. 4 (1999) 2387–2390.

[15] J. Couche, C. Fuller, Active control of power train and road noise in the cabin of a sport utility vehicle with advanced speakers, *Proc. 1999 Int. Symp. Active Control of Sound and Vib*., Ft. Lauderdale, FL, (1999) 2–4.

[16] D. Otte, K. Fyfe, P. Sas, J. Leuridan, Use of principal component analysis for dominant noise source identification, In *Int. Conf., Adv. Control and Refinement of Vehicle Noise*, 1988, Birmingham, United Kingdom (No. 1988-2). (1988).

[17] R.J. Alfredson, The partial coherence technique for source identification on a diesel engine, *J. Sound Vib*. 55 (1977) 487–494.

[18] M.E. Wang, M.J. Crocker, On the application of coherence techniques for source identification in a multiple noise source environment, *J. Acoust. Soc. Am*. 74 (1983) 861–872.

[19] P.A. Nelson, S.J. Elliott, *Active Control of Sound*, Academic Press, 1991.

[20] D.C. Kammer, Sensor placement for on-orbit modal identification and correlation of large space structures, *J. Guid. Control Dyn*. 14 (1991) 251–259.

[21] D.C. Kammer, M.L. Tinker, Optimal placement of triaxial accelerometers for modal vibration tests, *Mech. Syst. Signal Process*. 18 (2004) 29–41.

[22] D.C. Kammer, Sensor set expansion for modal vibration testing, *Mech. Syst. Signal Process*. 19 (2005) 700–713.

[23] M. Meo, G. Zumpano, On the optimal sensor placement techniques for a bridge structure, *Eng. Struct*. 27 (2005) 1488–1497.

[24] D.S. Li, H.N. Li, C.P. Fritzen, The connection between effective independence and modal kinetic energy methods for sensor placement, *J. Sound Vib*. 305 (2007) 945–955.

[25] T. Kim, B.D. Youn, H. Oh, Development of a stochastic effective independence (SEFI) method for optimal sensor placement under uncertainty, *Mech. Syst. Signal Process*. 111 (2018) 615–627.

[26] S.S. Haykin, *Adaptive Filter Theory*, Pearson Education India, 2008.

[27] W.B. Ferren, R.J. Bernhard, Active control of simulated road noise, *SAE Trans*. (1991) 1411–1424.

# 국 문 초 록

노면소음은 차량 NVH 성능에 직접적인 영향을 미치는 주된 소음원이다. 능동소음제어(ANC) 기술은 타이어와 도로 간의 상호작용으로 인한 차량 내부 소음을 감소시키는 유망한 솔루션이다. 노면소음 능동제어(ARNC) 시스템에는 노면소음을 유발하는 진동을 취득하기 위한 가속도 센서 세트가 포함되며, 진동 전달 경로를 정확하게 파악하기 위해 가속도 센서의 위치가 중요하다. 따라서 ARNC 시스템의 성능을 극대화하기 위해서는 후보 센서들 중에서 최적의 센서 세트를 찾아야 한다. 가능한 모든 센서 조합을 시뮬레이션 하는 시행착오 방법은 많은 시간이 소요된다. 본 논문에서는 상관성 분석 및 피셔 정보행렬을 사용하여 참조 센서 위치 집합을 결정하는 방법을 제안한다. 이 방법론은 출력 음압 수준 신호와 상관관계가 가장 높은 하나의 센서에서 시작한다. 초기 센서 세트는 상관성 정보행렬의 행렬식을 극대화하여 원하는 센서 개수까지 반복적으로 확장된다. 이 접근 방식은 계산량을 상당히 감소시켜 소요시간을 단축할 수 있다. 또한 이 기법을 적용하여 얻은 결과는 약 7 dBA의 광대역 노면소음 감소를 나타내었고, 모든 주행조건에서 목표 소음 감소 결과의 0.2 ΔdBA 이내의 오차를 보였다.

**주요어 : 노면소음 능동제어, 최적 센서 배치, 유효 독립성 기법, 상관성 함수, 피셔 정보행렬**

**학 번 : 2019-22509**